

Higgs Searches at the Tevatron

Gavin Davies, on behalf of the CDF and DØ collaborations

Imperial College London, SW7 2AZ

Abstract. The CDF and DØ experiments have carried out a wide range of Higgs searches, using an integrated luminosity of up to 2.4 fb^{-1} . As no significant excess of signal above the expected background is observed in any of the various final states examined, limits at 95% confidence level (CL) are presented.

Keywords: Higgs, searches, Tevatron

PACS: 14.80.Bn, 14.80.Cp

INTRODUCTION

The Higgs mechanism breaks electroweak symmetry within the Standard Model (SM) by introducing a scalar field to generate particle masses. The existence of an additional neutral particle (the Higgs boson) is also predicted, though its mass is not. Direct searches at LEP II have excluded a SM Higgs boson with mass below 114 GeV at 95% CL. Indirect constraints from precision measurements, including Tevatron results on the top and W mass, favour a light Higgs, with a mass below 190 GeV at 95% CL including the LEP II exclusion [1].

Standard Model Higgs production at the Tevatron is dominated by gluon fusion, with smaller contributions from associated production with a W or Z boson. Cross sections are of order 0.1 to 1 pb. At low mass (below 135 GeV) the dominant Higgs decay mode is to $b\bar{b}$, so searches use associated production to avoid the huge SM background to the gluon fusion production. Above 135 GeV decays to WW^* dominate, and gluon fusion production can be utilised.

Many models beyond the SM, including Supersymmetry, predict larger Higgs production cross sections, some within reach even with the present data sets. The Minimal Supersymmetric extension of the SM (MSSM) introduces two Higgs doublets and so contains five physical Higgs bosons [2]. Two of them are CP-even scalars, h and H , of which h is the lighter and SM-like. The other three consist of a charged Higgs pair, H^\pm , and a CP-odd pseudo-scalar, A , the mass of which is one of the two free parameters of the model at tree level. The production cross section of the Higgs in the MSSM is proportional to the square of the second free parameter of the model, $\tan\beta$, the ratio of the two vacuum expectation values of the Higgs doublets. Large values of $\tan\beta$ thus result in significantly increased production cross sections compared to the SM. Moreover, in the large $\tan\beta$ limit one of the CP-even scalars and the CP-odd pseudo-scalar are degenerate in mass, leading to a further

cross section enhancement. The main production mechanisms for such neutral Higgs bosons are the $gg, b\bar{b} \rightarrow \phi$ and $gg, q\bar{q} \rightarrow \phi + b\bar{b}$ processes, where $\phi = h, H, A$. The branching ratio of $\phi \rightarrow b\bar{b}$ is around 90% and $\phi \rightarrow \tau^+\tau^-$ is around 10%. More exotic scenarios including fermiophobic models with enhanced Higgs decay to $\gamma\gamma$ or WW and doubly-charged Higgs production have also been searched for.

This note summarises the analyses presented at SUSY08, based on an integrated luminosity of up to 2.4 fb^{-1} . More information, along with the latest results, is available from the public pages of CDF and DØ [3, 4].

STANDARD MODEL

High Mass: $gg \rightarrow H \rightarrow WW^*$

Both CDF and DØ search in the di-lepton (ee , $\mu\mu$ and $e\mu$) modes, requiring oppositely-signed leptons with transverse momenta above 10-20 GeV depending upon the channel. To reduce backgrounds from Z/γ^* , moderate missing transverse energy ($\approx 20 \text{ GeV}$) is required. Vetoing events with at least two jets or high total jet energy reduces the top pair background. QCD processes, including semi-leptonic quark decays and jets faking electrons, are reduced by requiring lepton isolation and a di-lepton mass above $\approx 15 \text{ GeV}$. The remaining dominant background is SM WW production and the opening angle, $\Delta\phi(l, l)$, between the leptons is a powerful discriminant variable as the spin-0 Higgs tends to produce more collinear leptons. The $\Delta\phi(l, l)$ distribution from the DØ ee analysis in the RunIIb data sub-sample after basic cuts (preselection) is shown in Fig. 1.

To improve the sensitivity both experiments use artificial neural networks (NN). Kinematic variables formed from the lepton transverse momenta, missing energy and the angles between them are included. In addition matrix element (ME) inputs are used, typically in the form

of a likelihood ratio discriminant (LR) as shown below, constructed from the the matrix element probabilities for each selected event to be Higgs signal or background.

$$LR(x_{obs}) = \frac{P_H(x_{obs})}{P_H(x_{obs}) + \sum_i k_i P_i(x_{obs})} \quad (1)$$

where x_{obs} are the observed leptons and missing energy, P_H is the probability for one of the Higgs mass hypotheses, and k_i are the expected background fractions, with $\sum_i k_i = 1$. CDF calculate ME probabilities for the WW, ZZ, $W\gamma$ and W+jet processes, providing four inputs to the NN, whilst DØ currently use only the WW process, and a larger number of kinematic inputs. The shape of the NN output is used in both cases as the final discriminant variable. The NN output from CDF is shown in Fig. 2. As no significant excess is observed limits are set. The CDF and DØ observed limits are 1.6 and 2.1 times the SM cross section for a Higgs mass of 160 GeV, with expected limits of 2.5 and 2.4 respectively.

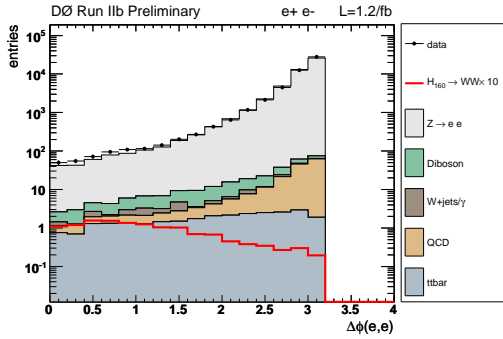


FIGURE 1. The $\Delta\phi(l,l)$ distribution from the DØ $H \rightarrow WW^*$ search.

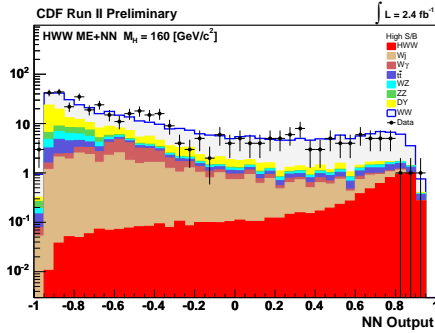


FIGURE 2. The NN output from the CDF $H \rightarrow WW^*$ analysis.

Low Mass: $WH \rightarrow lvb\bar{b}$

Below around 135 GeV, the Higgs decays primarily to $b\bar{b}$, and so associated production is used. Production in

association with a leptonically decaying W provides the most stringent constraints on a low mass Higgs. Both experiments use the electron and muon channels, with the basic selection requiring a single isolated lepton (≈ 15 -20 GeV), missing transverse energy (≈ 20 GeV) and two jets (≈ 20 GeV) which are then b -tagged. Identifying b -jets is crucial in this channel, as it is for all low mass SM Higgs searches. DØ uses a neural net tagger based on lifetime information giving high efficiency, 50-70%, for a mistag rate of 0.3-4.5% [5]. CDF use secondary vertex reconstruction, achieving efficiencies of 40-50% for a mistag rate of 0.5-1.5%. In addition, CDF applies a jet probability based b -tagger and NNs to separate heavy and light flavor jets depending on the analysis. To improve the overall sensitivity both experiments divide the analyses into orthogonal channels with different sensitivities e.g. single and double b -tag channels or central and forward leptons. The final event selections are NN based, with kinematic variables based on the objects in the event, e.g. lepton, jets, missing transverse energy, used as inputs. Two of the inputs, namely the missing energy imbalance and the invariant mass, as used by CDF and DØ are illustrated in Figs. 3, 4. The NN outputs are used as the final discriminant in both cases. CDF set a 95% CL limit corresponding to 8.2 times the SM cross section (7.3 expected) for a 115 GeV Higgs; the DØ 95% CL limits correspond to 10.9 times the SM cross section (8.9 expected) for a 115 GeV Higgs.

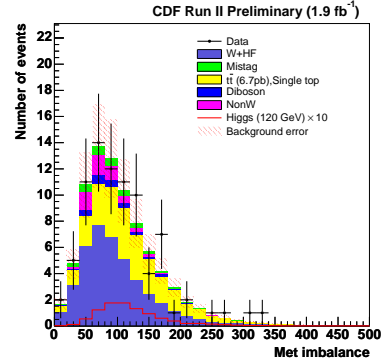


FIGURE 3. The missing transverse energy imbalance from the CDF $WH \rightarrow lvb\bar{b}$ analysis (double tag sample).

Recently CDF have increased their acceptance by 25% by including isolated tracks, from leptons that were not fully reconstructed. Including this class of events improves the expected limit at 115 GeV by 14%.

Low Mass: $ZH \rightarrow \nu v b\bar{b}$

Despite the large Z branching ratio to neutrinos this channel is experimentally very challenging. Events must be triggered on jets plus missing energy, and tight cuts

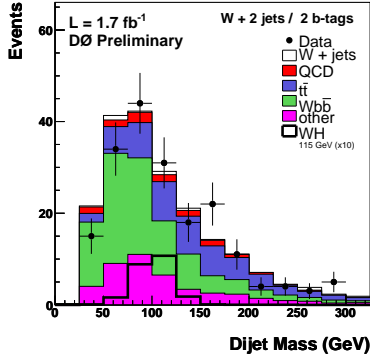


FIGURE 4. The invariant mass from the $DØ WH \rightarrow l\nu b\bar{b}$ analysis (double tag sample).

used to reject background. $DØ$ require two jets of at least 20 GeV, with CDF requiring one jet above 60 GeV and one above 20 GeV; both experiments require at least 50 GeV of missing energy, not aligned with the jets. The physics background shapes (Z+jet, top and di-boson) are taken from Monte Carlo. Understanding the remaining instrumental background, in the form of fake missing energy from mis-measured jets, remains the main challenge and is determined from data. Both experiments utilise the fact that for signal events the track derived missing energy should point in the same direction as the energy derived from the calorimeters, whilst in the case of mis-measurement it should not. $DØ$ develop a series of cuts based on this and the asymmetry of the missing energy as measured with all calorimeter cells and with jets whilst CDF use a neural network with track-based inputs. To maximise the final sensitivity CDF and $DØ$ use NNs and decision trees (DT) as the final discriminants. The DT output from the $DØ$ RunIIa sub-sample is shown in Fig. 5.

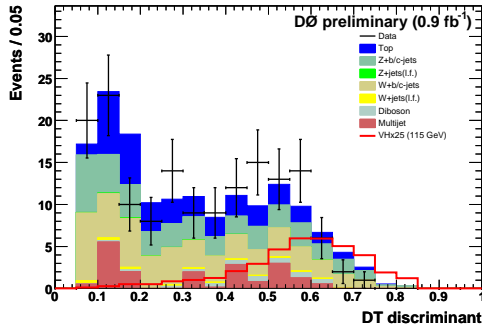


FIGURE 5. The RunIIa DT output distribution from the $DØ ZH \rightarrow \nu\nu b\bar{b}$ search.

The contribution from $WH \rightarrow l\nu b\bar{b}$ where the lepton is not reconstructed is included in both cases. $DØ$ sets a 95% CL limit corresponding to 7.5 times the SM

(8.4 expected) for a 115 GeV Higgs; the CDF limits correspond to 8.0 times the SM (8.3 expected) for the same mass point.

Low Mass: $ZH \rightarrow llb\bar{b}$

Higgs production with a Z boson has a lower cross section than associated production with a W, but the leptonic (e or μ) Z decays provide a clean Z signal, even with loose lepton requirements and p_T cuts (15 GeV is typical). Two jets are then required above 15 GeV ($DØ$) or one above 25 and one above 15 GeV (CDF). After this preselection, the dominant background of Z+jets events is reduced by b -tagging, with both experiments again forming orthogonal single and double-tagged channels. As there is no intrinsic missing energy in the signal events CDF assign missing transverse energy to the two Higgs candidate jets according to their missing energy projections and relative azimuthal angle, ϕ , using a NN. The output is a correction to each of the two jet energies. The corrected variables, along with additional kinematic information derived from them including the invariant mass, are used in a subsequent 2-D NN to separate signal from the two dominant backgrounds, namely Z+jets and $t\bar{t}$. $DØ$ also use a NN as the final discriminant variable, taking as input similar kinematic variables. No significant excess is again observed. The observed limits are 16 and 18 times the SM Higgs cross section for a 115 GeV Higgs for CDF and $DØ$ respectively, with expected limits of 16 and 20 times the SM prediction.

$WH \rightarrow WWW^*$ and additional channels

The process $WH \rightarrow WWW^*$ contributes at intermediate mass. Two like-sign leptons (ee , $\mu\mu$ and $e\mu$) with large transverse momenta (15 GeV is typical) are searched for. The dominant backgrounds are di-boson production and charge flips, with the latter being taken from data. CDF have recently released a cuts-based analysis with 1.9 fb^{-1} of data, complementing $DØ$'s earlier 1.0 fb^{-1} result which uses a 2-D likelihood as the final discriminant. Inputs to the likelihood include the momenta of the leptons, their opening angle, their invariant mass and the missing transverse energy. In the absence of a significant excess over background limits are set, with the best expected limit being 25 times the SM cross section for a 140 GeV Higgs ($DØ$).

Considerable effort has gone into optimising the existing channels, and their sensitivity is improving rapidly. A factor of 1.7 beyond the square root luminosity gain expected from statistics has been achieved since 2005. Additional sensitivity can be acquired by the inclusion

of new channels. DØ recently released the first results in the $gg \rightarrow H \rightarrow \gamma\gamma$ channel, with expected limits 45 times the SM cross section for a 120 GeV Higgs. Both this and the WWW^* searches mentioned above also have fermiophobic interpretations. CDF have for the first time recently released results in the $Z/W + H \rightarrow q\bar{q}b\bar{b}$ and $H \rightarrow \tau\tau$ channels. The expected limit for the former is 40 times the SM cross section at 120 GeV, whilst for the latter it is 25 times the SM prediction for a Higgs boson of mass 115 GeV. The minimum of three NNs is used as the final discriminant variable and is shown in Fig. 6.

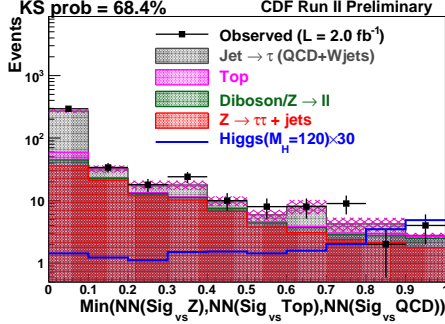


FIGURE 6. The final discriminant output from the CDF $H \rightarrow \tau\tau$ search.

While such sensitivities seem moderate, the $H \rightarrow \tau\tau$ result adds 10% to the CDF combination at low mass, and corresponds to 20% more data.

SM - Combination

The late spring 2008 Tevatron combination is shown in Fig. 7.

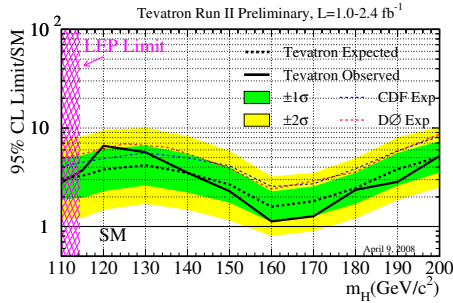


FIGURE 7. The observed and expected (median, for the background-only hypothesis) 95% CL upper limits on the ratios to the SM cross section, as a function of the Higgs boson test mass, for the combined CDF and DØ analyses.

In all 28 channels are combined across the two experiments. The signal-plus-background and background-only hypotheses are compared with Poisson likelihoods,

including the effect of systematics. Both Bayesian and Modified-frequentist methods are used, and found to be in good agreement. The observed (expected) limits at 115 GeV and 160 GeV are 3.7 (3.3) and 1.1 (1.6) times the SM prediction.

MSSM

$$\phi \rightarrow \tau^+ \tau^-$$

The reduced branching fraction for $\phi \rightarrow \tau^+ \tau^-$ is offset by the much reduced multijet background, allowing one to take advantage of the the inclusive $gg \rightarrow \phi$ production. CDF and DØ [6] have searched in the three channels, $e\tau_{had}$, $\mu\tau_{had}$, $e\mu$ where the τ decay products are indicated and τ_{had} indicates a hadronic τ decay, using datasets of 1.8 fb^{-1} and 1.0 fb^{-1} respectively. The signal is two high- p_T τ leptons, with missing transverse momenta in the same hemisphere as the e/μ and τ -candidate. The $W + \text{jets}$ background can be reduced by cutting on the transverse W mass and the azimuthal angle between the visible lepton and the missing transverse energy. Multijet backgrounds are estimated from orthogonal data samples. Tau identification at CDF is carried out using a variable cone-sized algorithm whilst DØ use a series of NNs depending upon tau-type. The final dominant background is $Z \rightarrow \tau^+ \tau^-$ and is estimated from Monte Carlo. Both experiments use the visible mass, $M_{vis} = \sqrt{(P_{\tau_1} + P_{\tau_2} + \cancel{P}_T)^2}$, calculated using the four-vectors of the visible tau decay products $P_{\tau_{1,2}}$ and of the missing momentum $\cancel{P}_T = (\cancel{E}_T, \cancel{E}_x, \cancel{E}_y, 0)$, as the discriminating variable. The CDF visible mass in the $e\tau_{had}$ and $\mu\tau_{had}$ channels combined is shown in Fig. 8.

Good agreement between data and expectation is observed. As no significant excess is observed in either experiment limits are set, initially in a model independent way on the production cross section times branching ratio. To take into account radiative corrections limits on $\tan\beta$ as a function of m_A are then set for the two standard scenarios: the m_h^{\max} scenario¹ and the no-mixing scenario². Figs. 9,10 show the resulting 95% CL exclusions in the $\tan\beta - m_A$ plane for some of the scenarios, for a positive value of μ ; the limits are very similar for a negative value. In the MSSM the width of the Higgs boson can become larger than in the SM. DØ included this effect, but as $\Gamma_A/m_A < 0.1$ for $m_A < 200$ GeV in these scenarios, the effect of the width is small.

¹ $M_{SUSY} = 1 \text{ TeV}$, $X_t = 2 \text{ TeV}$, $M_2 = 0.2 \text{ TeV}$, $\mu = \pm 0.2 \text{ TeV}$, and $m_g = 0.8 \text{ TeV}$.

² $M_{SUSY} = 2 \text{ TeV}$, $X_t = 0 \text{ TeV}$, $M_2 = 0.2 \text{ TeV}$, $\mu = +0.2 \text{ TeV}$, and $m_g = 1.6 \text{ TeV}$ where X_t is the mixing parameter, M_2 is the gaugino mass term, m_g is the gluino mass and M_{SUSY} is a common scalar mass.

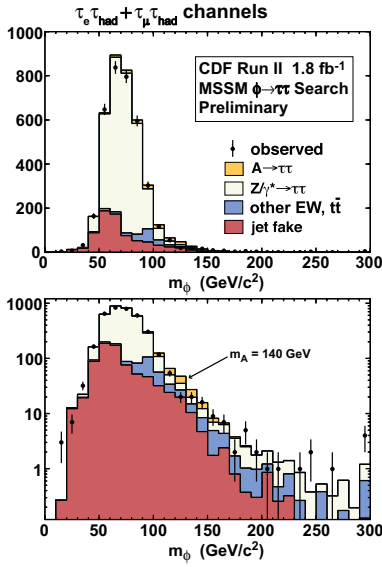


FIGURE 8. The visible mass in the combined $e\tau_{had}$ and $\mu\tau_{had}$ channels from CDF.

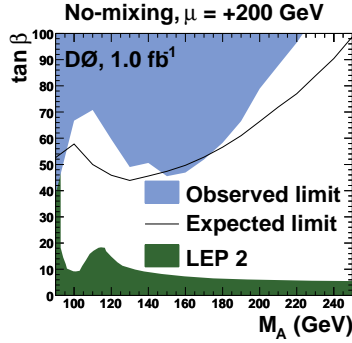


FIGURE 9. Excluded region in the $\tan\beta - m_A$ plane from $D\emptyset$ for a positive mass parameter in the $\phi \rightarrow \tau^+\tau^-$ analyses. Also shown is the LEP limit [8].

$$b\phi \rightarrow b\bar{b}$$

Though this channel has a very large branching ratio the large multijet background means that inclusive production can not be studied, and indeed understanding the background in this fully hadronic decay is the major challenge. CDF and $D\emptyset$ [7] have carried out searches in this channel in data samples of 1.9 fb^{-1} and 1.0 fb^{-1} respectively, looking for three b -tagged jets using the b -tagging algorithms described earlier. The signal corresponds to an excess over background in the dijet invariant mass formed from the two Higgs candidate jets. Though the requirement of a third b -tag reduces the QCD background, the so-called ‘3tag’ sample remains QCD dominated and its composition is determined using both simulation and data. Heavy flavour jets as well as mis-

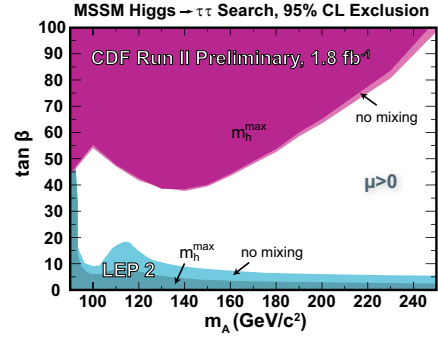


FIGURE 10. Excluded region in the $\tan\beta - m_A$ plane from CDF in the m_h^{max} and no-mixing scenarios for $\mu > 0$ in the $\phi \rightarrow \tau^+\tau^-$ analyses. Also shown is the LEP limit [8].

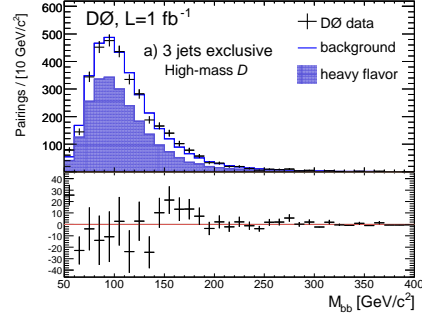


FIGURE 11. Invariant mass for the high-mass likelihood region for the exclusive three-jet channel. Black crosses refer to data, the solid line shows the total background estimate, and the shaded region represents the heavy flavour component ($b\bar{b}b$, $b\bar{b}c$, and $c\bar{c}b$). The lower panel shows the difference between the data and the background expectation. Only statistical errors are shown.

tagged light jets can contribute. CDF use dijet invariant mass and secondary vertex mass templates, whilst $D\emptyset$ use multiple b -tagging criteria with known efficiencies to determine the relative contribution of the different backgrounds. As the Higgs boson width can become considerably larger than the experimental resolution both experiments explicitly include this effect, with a consequent decrease in sensitivity at large values of $\tan\beta$ as the invariant mass spectrum is broadened. To increase sensitivity $D\emptyset$ include multiple possible Higgs’ jet-pairings, split the analysis into exclusive three-, four-, and five-jet samples and use a likelihood discriminant (tailored for either low or high mass) based on kinematic information. The invariant mass for the optimised high-mass likelihood cuts is shown in Fig. 11 for the exclusive 3-jet channel.

Again model independent limits on cross section are initially set before interpretation in the standard scenarios. This channel is more sensitive than the $\phi \rightarrow \tau^+\tau^-$ channel to the details of the radiative corrections

and so greater dependence on the scenarios is observed. Figs. 12,13 illustrate some of the exclusions in the $\tan\beta - m_A$ plane. The difference in the observed and expected limits on the $D\emptyset$ plots reflects the slight data excess around 180 GeV, also visible in Fig. 11.

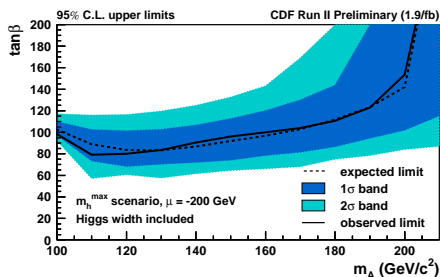


FIGURE 12. Excluded region in the $\tan\beta - m_A$ plane for a negative mass parameter μ in the m_h^{\max} scenario from CDF in the $b\phi \rightarrow b\bar{b}b$ analysis. Also shown is the LEP limit [8].

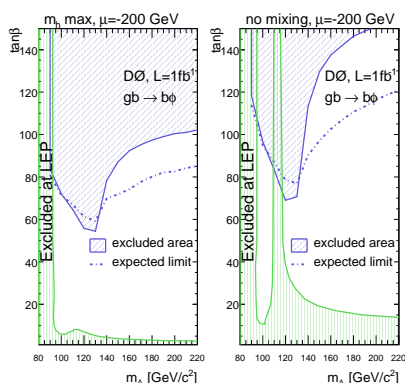


FIGURE 13. Excluded region in the $\tan\beta - m_A$ plane for a negative mass parameter μ in both scenarios from $D\emptyset$ in the $b\phi \rightarrow b\bar{b}b$ analysis. Also shown is the LEP limit [8].

In addition $D\emptyset$ has carried out searches for neutral Higgs bosons in the $b\phi \rightarrow b\tau^+\tau^-$ channel.

Furthermore searches for charged Higgs bosons, doubly-charged Higgs bosons and fermiophobic Higgs bosons have also been carried out by both experiments; for further details see the proceedings from the parallel sessions.

CONCLUSIONS

CDF and $D\emptyset$ have performed searches for the SM and non-SM Higgs bosons over a range of masses with an integrated luminosity of up to 2.4 fb^{-1} . No significant excess over expected background was observed, so limits were set.

The Tevatron combined SM limit shown in Fig. 7 illustrates how the Tevatron is closing-in on the needed sensitivity, in particular at high-mass where we are only

a factor of ≈ 1.5 from the Standard Model. First exclusion is hoped for here in the summer 2008 conferences. Overall sensitivity has increased significantly faster than the expected statistical gain from increased luminosity through, amongst other things, improved trigger efficiency, lepton acceptance, b -tagging and multivariate techniques. Further improvements, particularly at low mass, are foreseen. Incorporating such gains, by the end of 2010 running, exclusion over virtually the full mass range favoured by the electroweak fits is achievable. In addition three sigma evidence will be possible over much of the same range.

The searches for non-SM Higgs bosons also show very promising sensitivity and have already produced new powerful limits, particularly on $h/H/A \rightarrow \tau\tau/b\bar{b}$. As well as new individual results, work will focus on combining the results from the different channels and across experiments, as well as improvements to the analyses themselves, as discussed for the SM case.

We are confidently looking forward to exploring the almost 4 fb^{-1} of data per experiment which has already been written to tape, and the 8 fb^{-1} total per experiment expected by the end of Run II.

ACKNOWLEDGMENTS

I would like to thank my colleagues from the CDF and $D\emptyset$ Collaborations for providing material for this talk and the organisers of SUSY08 for a very interesting conference.

REFERENCES

1. <http://lepewwg.web.cern.ch/LEPEWWG/>
2. Dimopoulos S and Georgi H 1981 *Nucl. Phys. B* **193** 150
3. <http://www-cdf.fnal.gov>
4. <http://www-d0.fnal.gov>
5. Scanlon T *FERMILAB-THESIS 2006-043*
6. $D\emptyset$ Collaboration *Phys Rev. Lett.* **101** 071804
7. $D\emptyset$ Collaboration *arXiv:0805.3556 [hep-ex]* Submitted to *Phys Rev. Lett.*
8. Schael S *et al.* 2006 *Eur. Phys. J. C* **47** 547-587